

Supplemental Information, Voss et al.

Dynamic Exchange at Regulatory Elements during Chromatin Remodeling

1. Supplemental Data

Supplemental Figure 1. Shows the subnuclear localization of the receptors utilized in Figure 1, .

Supplemental Figure 2. Characterization of the receptors; expression levels, physical properties; related to Figures 1 and 2.

Supplemental Figure 3. Further examples of the two classes of chromatin organization near GREs, de novo and preprogrammed sites; related to Figure 4.

Supplemental Figure 4. A,B Demonstration that ER pbox protein produces inefficient chromatin access at MMTV. C, ReChIP of ER on GR primary ChIP. D, Retention of receptor in nucleus; all related to Figure 5.

Supplemental Figure 5. Examples of cJun assisted loading by GR; related to Figure 5.

Supplemental Figure 6. Description of the Monte Carlo simulation, related to Figure 6.

Supplemental Table 1. Assisted loading of ERpBox at endogenous GREs, related to Figure 4.

2. Supplemental Experimental Procedures

Restriction Endonuclease Accessibility Assay

Method to measure access to MMTV chromatin

3. Supplemental References

1. Supplemental Data

Supplemental Figure 1. Subnuclear localization of the receptors following different

hormone treatments. Related to Figure 1. (A-D) 6644 cell line cultures were treated for 30 minutes with the indicated hormones, then processed for RNA FISH to detect transcription from the MMTV array. Each row of micrographs displays a single nucleus with each fluorescence channel shown separately and merged in the overlay. (E) Fluorescence recovery after photobleaching (FRAP) experiments were performed on living 6644 cells following 30 minutes of treatment with E2. The micrographs show the bleaching of the specific subnuclear region that contains the Ch-ER pbox protein, which is concentrated at the MMTV array. (F) The graph shows the mean of quantification of the fluorescence recovery following the bleach. Error bars denote SEM of three randomly selected cells.

Supplemental Figure 2. Relative expression levels of endogenous steroid receptors and

exogenous fusion proteins. Related to Figures 1 and 2. Cultures of the 3617 cell line, the 6644 cell line, and the 7281 cell line were grown in the absence of tetracycline for 48 hours to

induce expression of the GFP-GR and Ch-ER pBox. Whole cell lysates were assayed by western blot using (A) anti-GR or (B) anti-ER primary antibody. (Middle) Molecular weight markers are shown. (Right panels) Ponceau S stain was performed to assess sample loading uniformity. © The primary amino acid structure of GR and ER are shown with domains indicating Activation Function 1 (AF1), DNA Binding Domain (DBD), Ligand Binding Domain (LBD), and Activation Function 2 (AF2). (D) The individual amino acids are diagramed for the Estrogen receptor proximal zinc finger. Three amino acid changes (pBox mutations) cause the ER pBox mutant protein to interact with the GRE consensus sequence instead of the ERE consensus sequence. (E) Although the GRE and ERE are similar, there are distinct nucleotide requirements (boxed) for specific receptor interaction that are located in each half-site of the consensus elements. (F) An automated image analysis algorithm measures the fraction of the cell population displaying strong receptor/MMTV steady-state binding. The example images shows two adjacent cell nuclei, only one of the two cells has GR concentrated visibly at the MMTV array, which is automatically detected by the algorithm (red region of interest in the area magnified in the yellow box). (G) Example images of 7438 cell line nuclei expressing GFP-GR and mCh-ER wild type. Results of image analysis measuring the concentration at the MMTV array by (H) GFP-GR and (I) Ch-ER wild-type or RNA FISH signal in the 7438 cell cultures. (K-L) Using the same image analysis algorithm, non-competitive GRE binding is detected in 6644 cell cultures.

Supplemental Figure 3. Two distinct classes of chromatin organization near GREs.

Related to Figure 4. Genome-wide measurements of chromatin accessibility and GR/chromatin binding were obtained from the 3134 cell line as previously described (John et al., 2011). Example genome browser representations of this data are shown (A-E) for chromatin regions that are inaccessible prior to Dex treatment, but are remodeled as GR binds (*de novo*), and (F-I) for chromatin regions that are remodeled and open prior to receptor binding (preprogrammed). See Supplemental Table 1 for numerical values corresponding to the genome browser tracks. Y-axis values represent tag densities for sequence tags recovered from deep sequencing of DHS fragments, or ChIP-seq analysis of GR distributions.

Supplemental Figure 4. GR-dependent chromatin remodeling leads to increased binding of ER pBox protein to the same GR binding site. Related to Figure 5. ER pbox protein produces less chromatin access compared to GR protein. (A) Diagram details the endonuclease accessibility assay used to measure chromatin remodeling at the MMTV LTR. A SacI site cuts at the B-nucleosome region near GREs that regulate MMTV LTR-dependent transcription. *In vivo* Sac I chromatin accessibility is monitored by quantitative PCR amplification of the genomic DNA containing the Sac I site (Mulholland et al., 2003). Another region of the flanking chromatin is also measured by qPCR as a normalization control. (B) Quantification of Sac I assay results from cells treated for 30 min with no hormone, Dex or E2. Results are the mean of three independent experiments and error bars denote sem. © Re-ChIP experiments confirm that protein-protein interactions are not directly responsible for ER-pBox assisted loading. Cultures of 6644 cells were treated with the indicated hormones for 30 minutes, and prepared for re-ChIP assays using the indicated combinations or anti-bodies. Re-ChIP assays were evaluated by RT-PCR for the MMTV locus, and precipitated amounts of chromatin are shown relative to the input chromatin samples. (D) Retention of GR in nuclei during the isolation procedure. Cells (3134) were treated for 1 hr. with dex, and nuclei isolated under salt conditions used in the DHS protocol. GR was immunoprecipitated [sc1002 rabbit polyclonal (Santa Cruz)] from cytosolic and nuclear protein, and equal fractions were applied to a tris-glycine polyacrylamide (4-20%). After resolution, proteins were transferred to a membrane, and GR detected by western analysis [sc8992 rabbit polyclonal (Santa Cruz)]. The vast majority of receptor remains in the nucleus.

Supplemental Figure 5. GR-directed assisted loading of the cJun transcription factor. Related to Figure 5. Twenty-four examples are presented (panels A and B) for assisted loading of cJun at GR *de novo* sites. Chromatin accessibility was determined by the DNaseI-seq assay; GR and cJun binding by ChIP-seq (John et al., 2011). Tag densities are plotted vs. genome coordinate (NCBI36/mm8) for cJun ChIP - dex (light blue), + dex (green); DHS -dex (blue), +dex (purple); and GR + dex (red). Green arrows indicate cJun binding events that result from GR induced chromatin opening (purple arrows).

Supplemental Figure 6. Monte Carlo simulation of transient GR/GRE interactions.

Related to Figure 6. At the beginning of each time step, an individual GRE is either unoccupied, or occupied by receptor. Thus, each GRE is in one of two states. (A) The chance of changing states at each time step is determined by a random number generator and simulated association and dissociation probability constants. (B) To model the system over time the model is allowed to equilibrate for 400 time steps, then measurements are monitored for 600 time steps, modeling 60 seconds in the cell nucleus. © All time course calculations are repeated 1000x, simulating the behavior of the cell population. (D, E) Stair plots show Monte Carlo simulations of receptor(s) binding to a single GRE over a 60 sec time period. As specified for each panel, transitions between bound and unbound GRE state are random and dictated by two probabilities, “on” and “off”. Random transitions were calculated every 0.1 sec time step. The mean parameter values are shown for 1000 GRE simulations, calculated from the stair plot conditions.

Supplemental Table 1. Details of DHS and ChIP measurements at endogenous GREs.

Related to Figure 4 and Figure S3. 1A. Internal genomic locus identification numbers 1-15 match those listed in main figure 4 A,B and Figure S3A and S3B (Top) Genome-wide DHS measurements were obtained from the 3134 cell line treated for 30 minutes with no hormone (NH) or Dexamethasone (Dex), [see (John et al., 2011) for experimental details]. ChIP qPCR measurements were obtained from the 6644 cell line treated for 30 minutes with Dex alone, E2 alone or a combination of Dex and E2. Quantification of each specific chromatin immunoprecipitation qPCR amplification is listed relative to the amplification of the no-antibody background qPCR amplification. (Bottom) Details of the primers used for qPCR quantification of ChIP experiments and the genomic regions that were examined. 1B. Additional examples: sites presented in 1B represent *de novo* DHS elements, that is, sites where chromatin opening is initiated by the glucocorticoid receptor. Also, each data point represents one biological replicate, whereas the data points in 1A are derived from biological triplicates. Assisted loading of the ERpBox protein is observed for all the sites presented in 1B.

2. Supplemental Experimental Procedures

Restriction Endonuclease Accessibility Assay

Restriction endonuclease cleavage of MMTV chromatin was performed as previously described (Mulholland et al., 2003). Briefly, isolated nuclei were digested with SacI. DNA was then purified and digested to completion with DpnII. Digestion products were amplified by primer extension with Taq polymerase and radiolabeled primer (see Supplemental Fig. 4). Extension products were analyzed on an 8% denaturing sequencing gel. Nuclease hypersensitivity was expressed as % fractional cleavage.

GR Levels in Isolated Nuclei

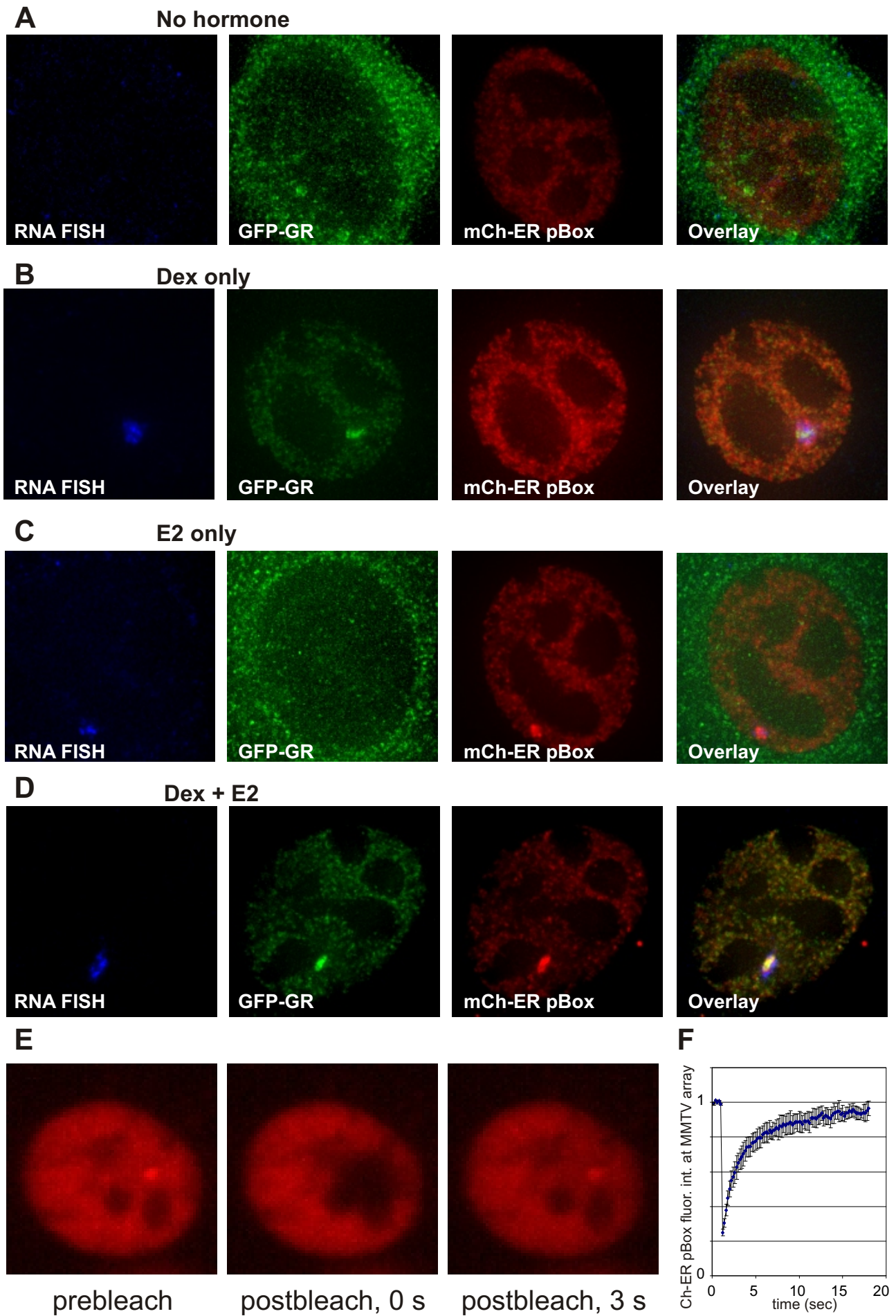
The level of GR retained in nuclei after fractionation was determined by immunoprecipitation. Nuclei and cytoplasmic fractions were prepared from 3134 cells treated for 20 min with hormone. After immunoprecipitation with GR antisera [P-20; sc1002, rabbit polyclonal (Santa Cruz)], GR levels were detected by western blot with antisera [H-300; sc 8992, rabbit polyclonal (Santa Cruz)].

3. Supplemental References

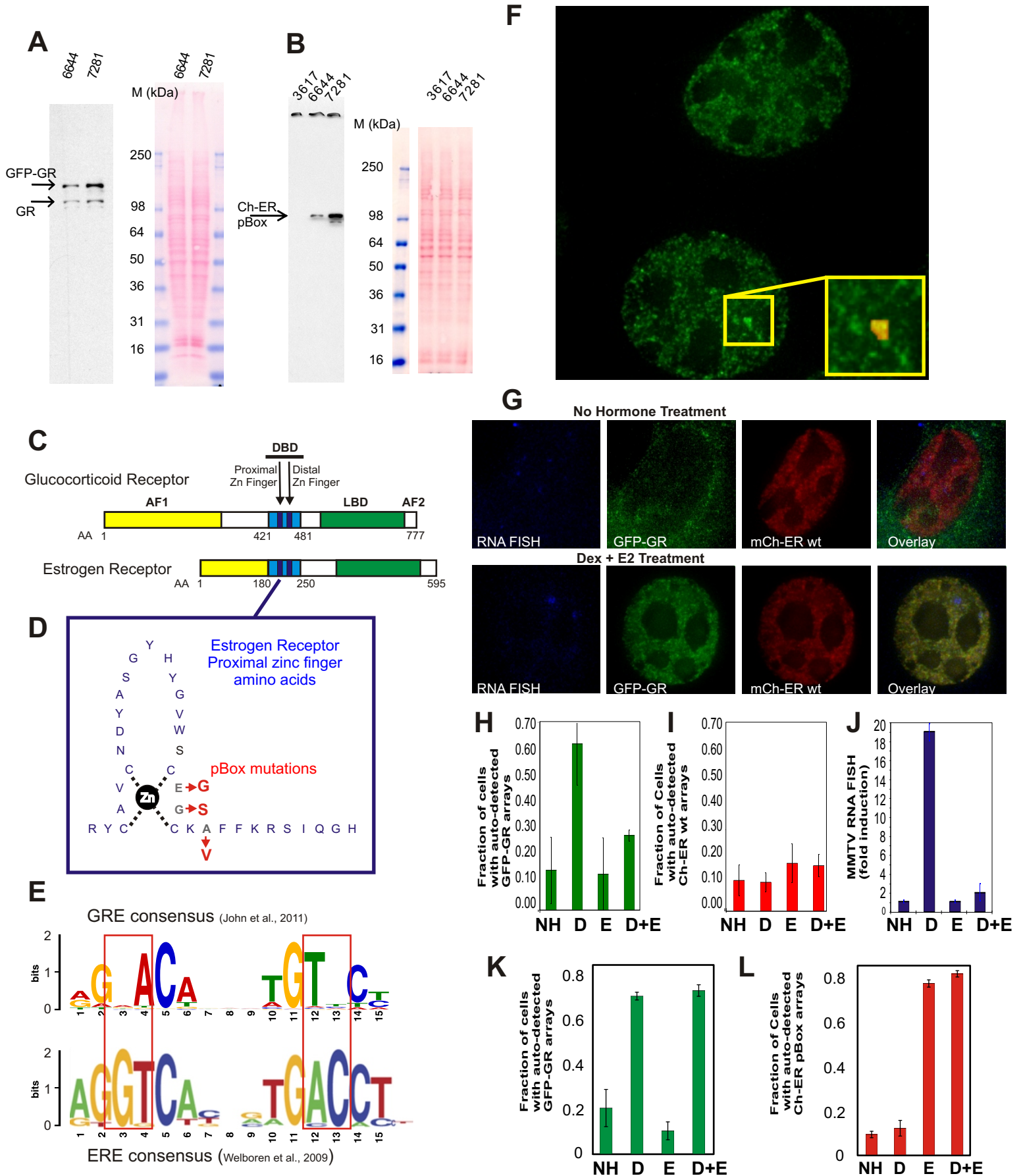
John,S., Thurman,R.E., Sabo,P.J., Sung,M.H., Biddie,S.C., Johnson,T.A., Hager,G.L., and Stamatoyannopoulos,J.A. (2011). Chromatin accessibility dictates de novo regulatory factor binding. *Nat. Genet.* 43, 264-268.

Mulholland,N.M., Soeth,E., and Smith,C.L. (2003). Inhibition of MMTV transcription by HDAC inhibitors occurs independent of changes in chromatin remodeling and increased histone acetylation. *Oncogene* 22, 4807-481.

Voss et al., Sup Fig 1



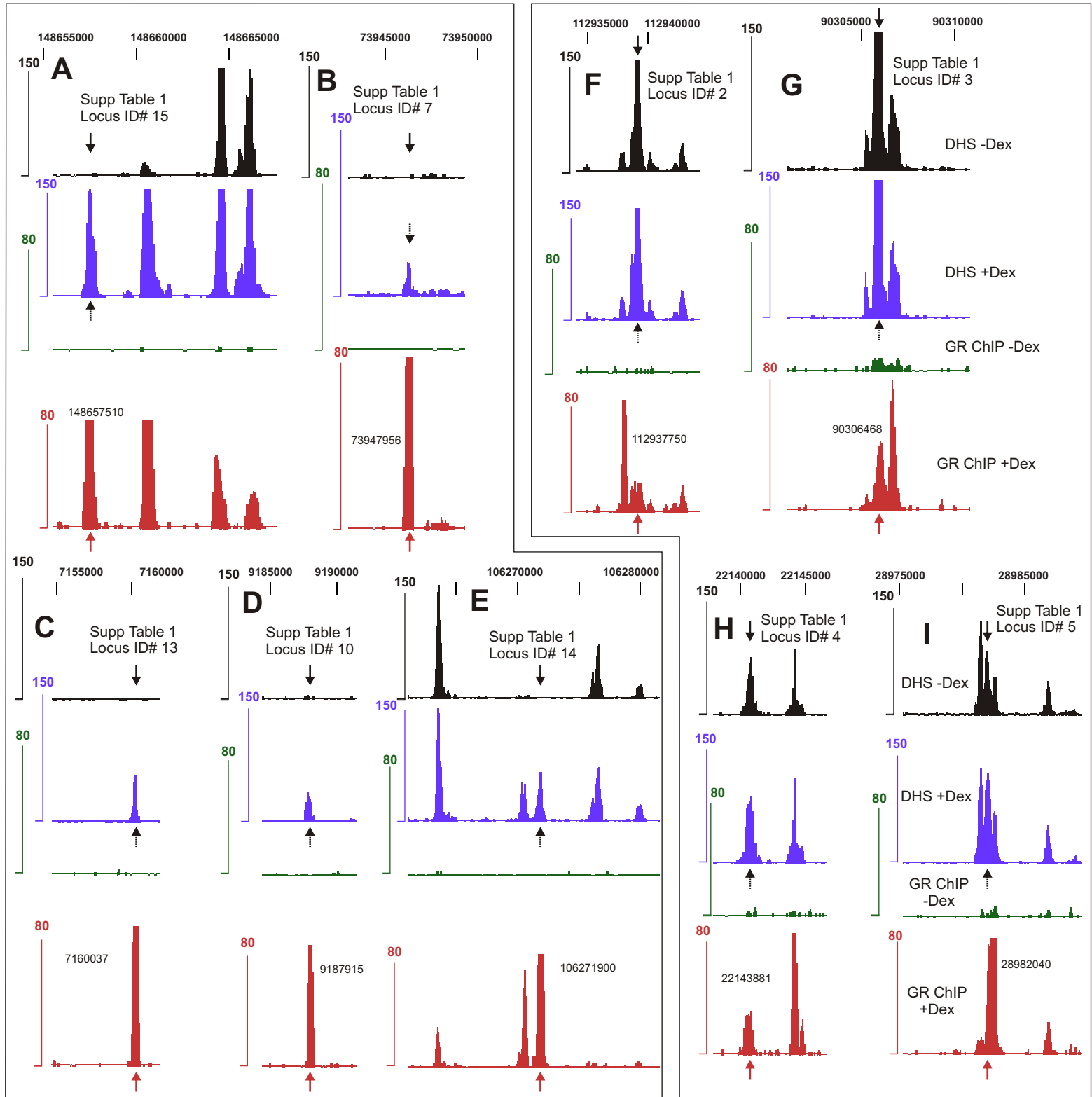
Voss et al. Supp Fig 2



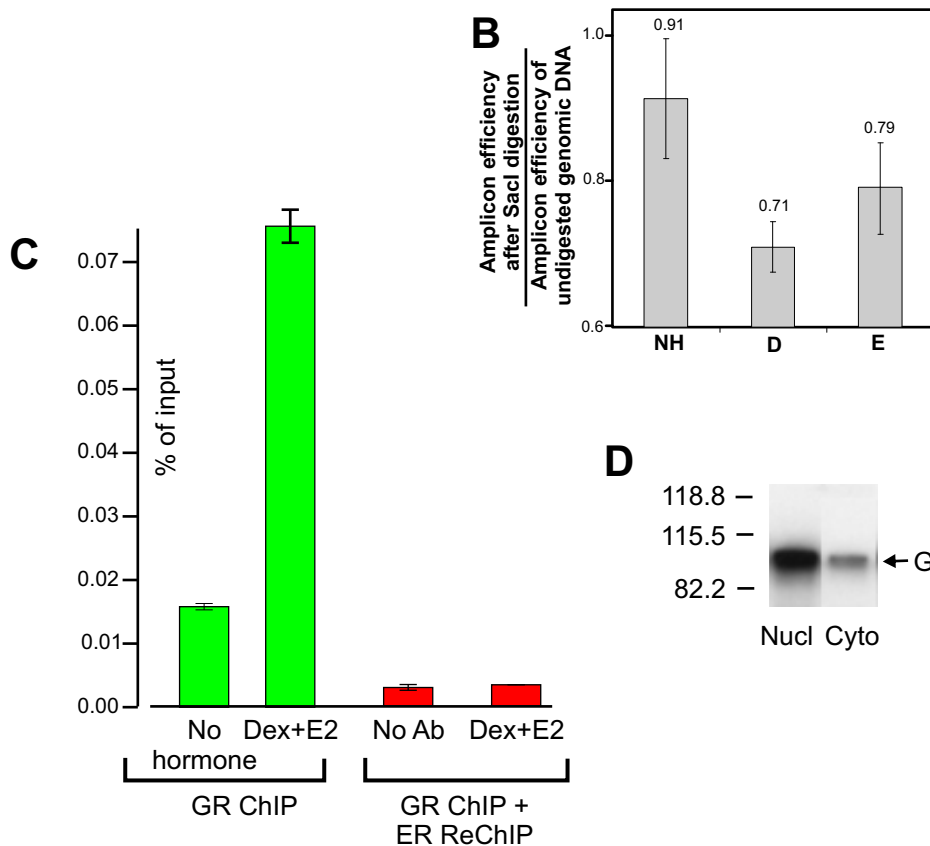
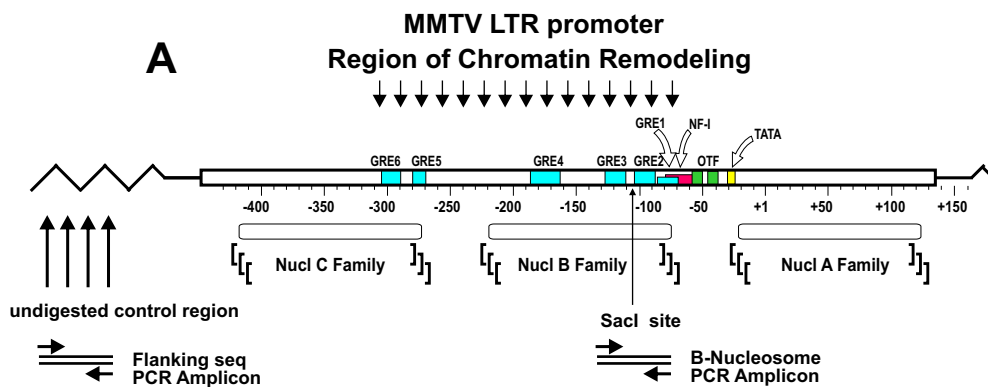
Voss et al. Supp Fig 3

de novo

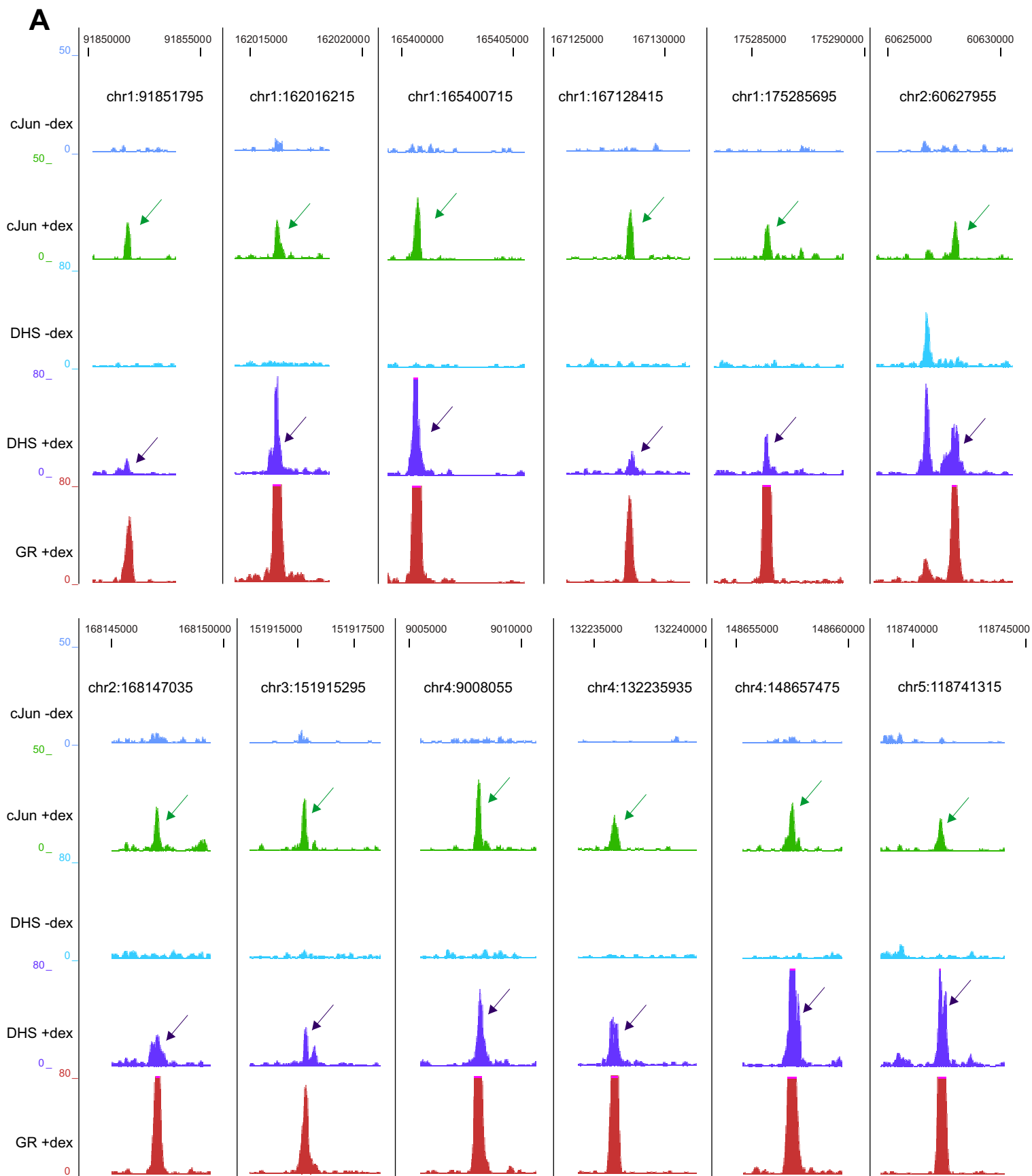
Pre-programmed



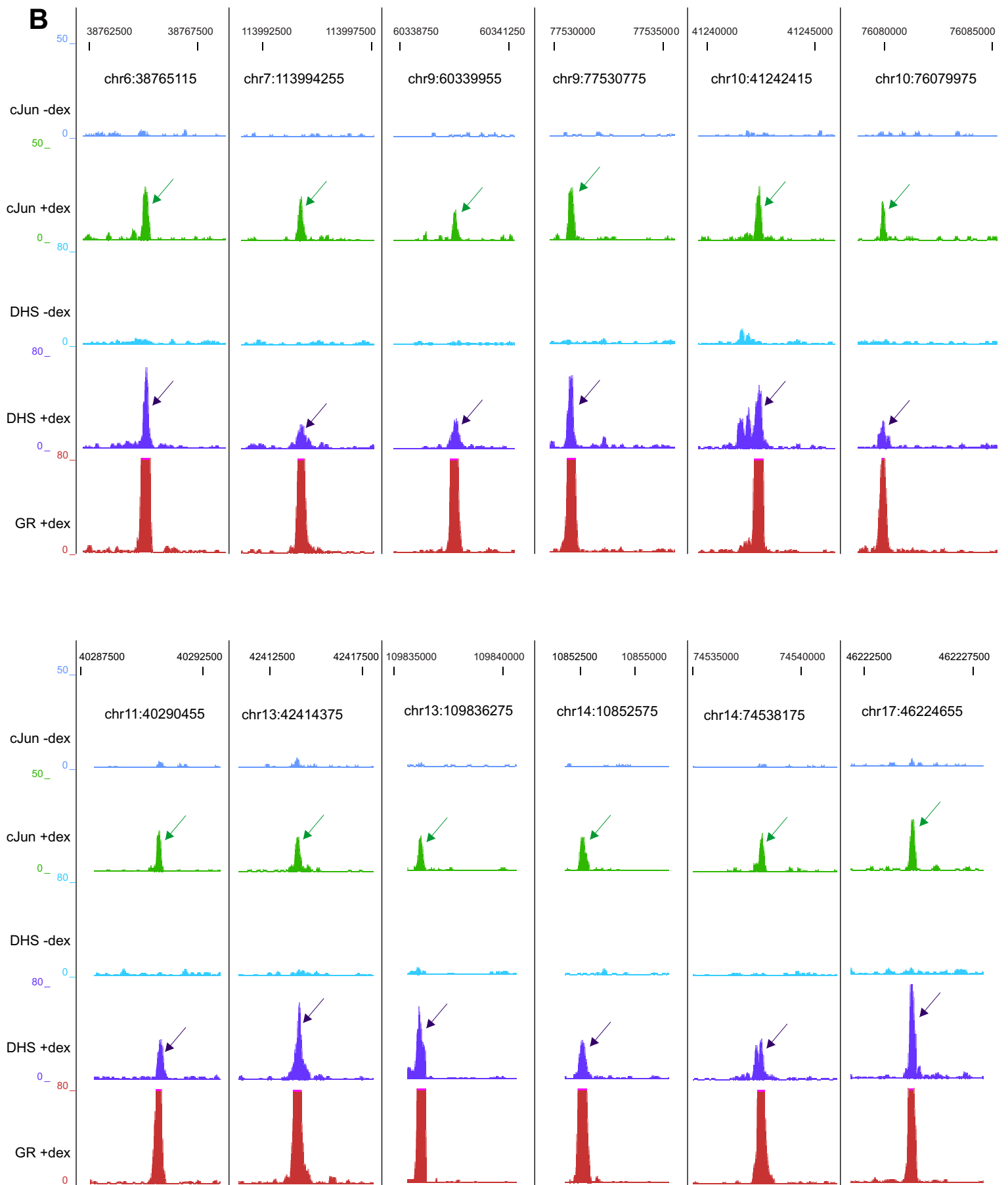
Voss et al., Supp Fig 4



Voss et al., Supp Fig 5

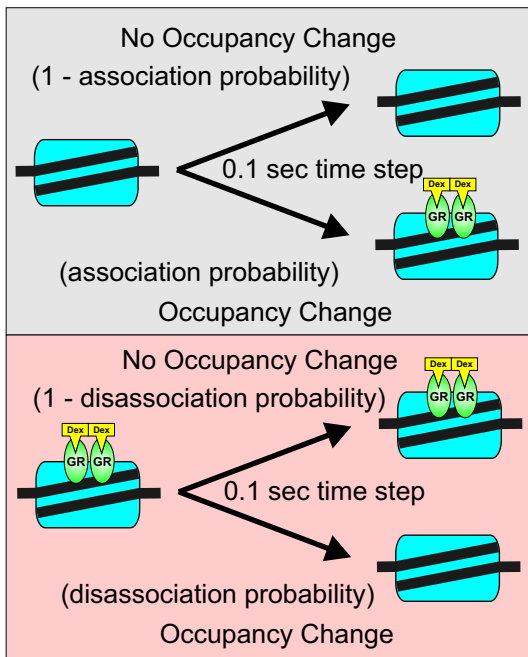


Voss et al., Supp Fig 5

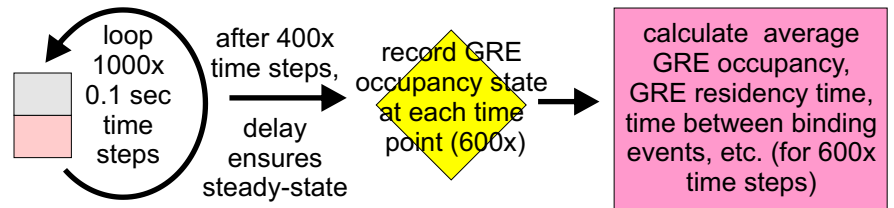


Voss et al., Supp Fig 5

A Stochastic state-change calculation module



B Single GRE occupancy over time calculation module



C GRE population average calculation module

